2011 5th COASTAL ALTIMETRY WORKSHOP
San Diego, U.S.A, 16-18 October 2011

Radar Altimetry Waveform Retracking Applied to Coastal Ocean

Kuo-Hsin Tseng[1], C.K. Shum[1], Yi Chao[2], William J. Emery[3], Hoksum Fok[1], Hyongki Lee[4], Chungyen Kuo[5], Yuchan Yi[1]

[1]Divison of Geodetic Science, School of Earth Sciences, The Ohio State University, Columbus, Ohio 43210, USA. tseng.95@osu.edu, ckshum@osu.edu, fok.8@osu.edu, yi.3@osu.edu
[2]Jet Propulsion Laboratory/Cal Tech., USA. Yi.Chao@jpl.nasa.gov; [3]CCAR, University of Colorado, USA. William.Emery@colorado.edu;
[4]Dept. of Civil & Environmental Eng., Univ. of Houston, USA. hlee@uh.edu; [5]National Cheng Kung University, Taiwan. kuo70@mail.ncku.edu.tw

1. Introduction

Measuring sea surface height at coastal and shallow (<200m in depth) water region has long been a challenge for researchers since the radar altimeter waveform is contaminated by complex topographic surfaces and shorelines, as well as, stronger ocean dynamics including tides, resulting in much less accurate measurements if the altimeter is still on-lock. The land effect induces additional peaks in the altimeter waveform that distorted from theoretic Brown's model as the ground footprint (radius ~7km at 1Hz sampling) approaching (or leaving) the shoreline. These peaks need to be edited in the waveform to avoid an error in the determination of leading edge and associated retracked gate while applying threshold retracking. Here, we introduce an algorithm to modify coastal waveforms (1~7km from coasts, and up to 20Hz) and use 20% threshold retracking method to correct the unretracked ocean surface height at four study areas (Fig.1). The measurements within 10km near shore used to hardly be allowed by conventional retrackers.

2. Method

Waveforms at deeper ocean region (20~30km) are used in each pass as a reference (Eq.1) for coastal (<7km) waveforms to remove additional peaks (Eq. 2), which are considered as returned from non-marine surface.

$$P_{ref}(i)=\frac{1}{k}\sum_{k=20km}^{30km}P_k(i)\ ,\quad i=\begin{cases}1\sim128 \text{ for Envisat}\\ 1\sim104 \text{ for Jason-2}\end{cases} \qquad .....(1)$$

where i = waveform gate, P_{ref} = reference waveform

k = number of waveforms between 20~30km from coasts

The flawed waveform is then repaired by a 2D linear interpolation both horizontally (nearby waveform gates) and vertically (same gate at nearby measurements) (Eq.3).

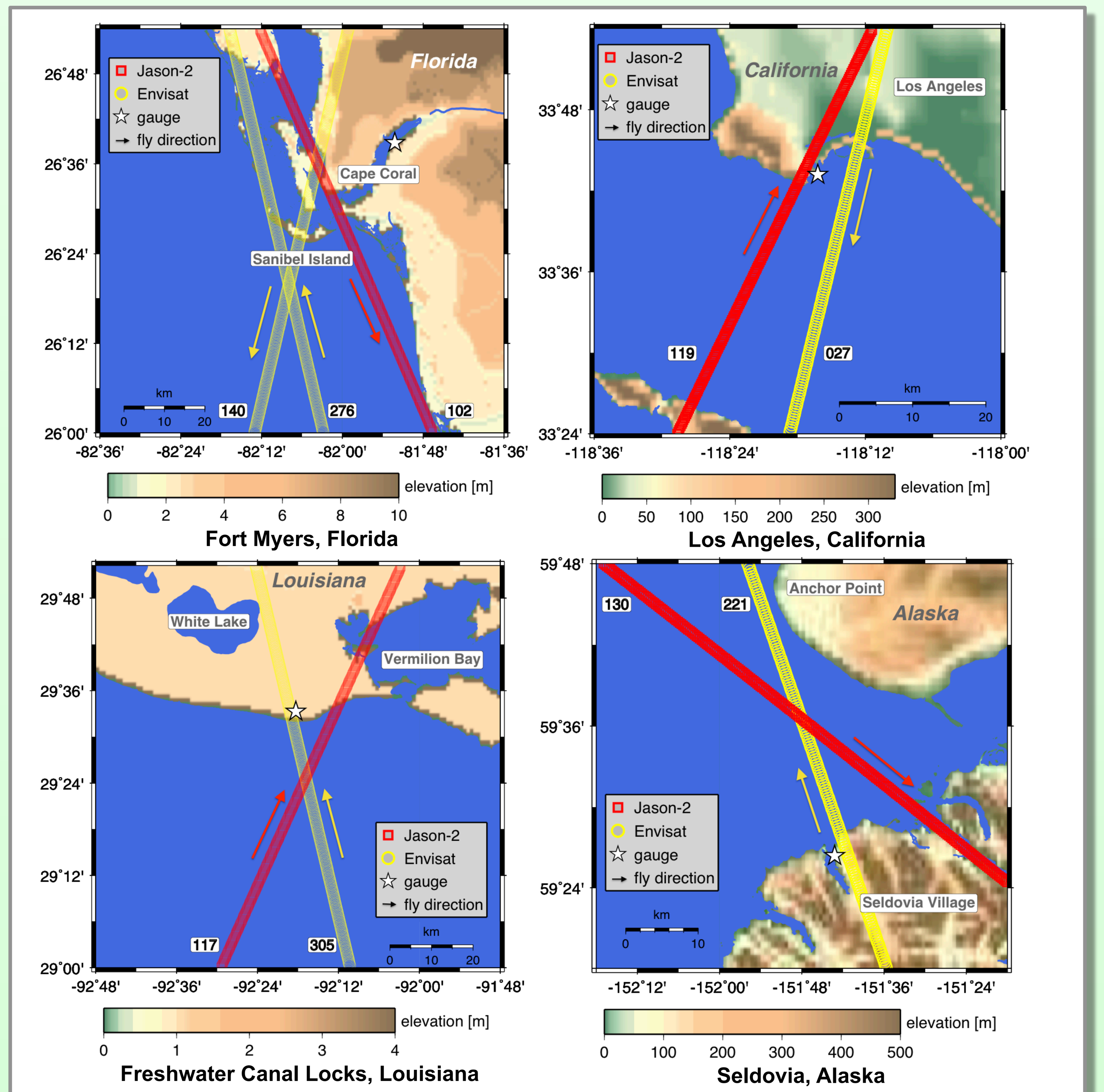

Figure 1. Four study areas (including satellite passes and gauge locations)

$$P_c(out)\in\left|P_c(i)-P_{ref}(i)\right|>2\sigma\ ,\quad i=\begin{cases}1\sim128 \text{ for Envisat}\\ 1\sim104 \text{ for Jason-2}\end{cases} \qquad .....(2)$$

where P_c = coastal waveform (<7km), $P_c(out)$ = gate outliers in coastal waveform

σ = standard deviation of $P_c(i)-P_{ref}(i)$

$$\bar{P}_c(out)=\frac{1}{2}\left[\left(\frac{P_c(out+1)+P_c(out-1)}{2}\right)+\left(\frac{P_{c+1}(out)+P_{c-1}(out)}{2}\right)\right] \qquad .....(3)$$

In addition, we apply a energy compensation correction for repaired waveform based on the reference waveform (Eq.4).

$$\hat{P}_c(i)=\bar{P}_c(i)\times\sum_{i=a}^{b}P_{ref}(i)\Big/\sum_{i=a}^{b}\bar{P}_c(i)\ ,\quad a=\begin{cases}42\\31\end{cases};\ b=\begin{cases}128 \text{ for Envisat}\\104 \text{ for Jason-2}\end{cases} \qquad .....(4)$$

This correction is necessary because the total return energy is limited by Automatic Gain Control (AGC) loop in the onboard altimeter. Once the extra high return signal existed in the waveform has been removed, the remaining bins following noise level are underestimated and need to be lifted to a similar level to the reference waveform. This process slightly change the slope of leading edge and the associated retracked gate.

Finally, we compute an averaged height between 1~7km for each pass and compare with nearby tide gauge 6-minute* water level data.

* Data available from NOAA (http://tidesandcurrents.noaa.gov/index.shtml)

3. Processing example

Fig.2 demonstrates waveform modifying process on Envisat cycle #91 pass #305 near Freshwater Canal Locks gauge station. This ascending pass started receiving land return signal at 7km from coasts. The additional peak in 2D view of side-by-side waveforms (lower right panel) migrated from the edge of footprint (end of trailing edge) to nadir (nominal tracking gate #46) as measurements move toward shoreline.

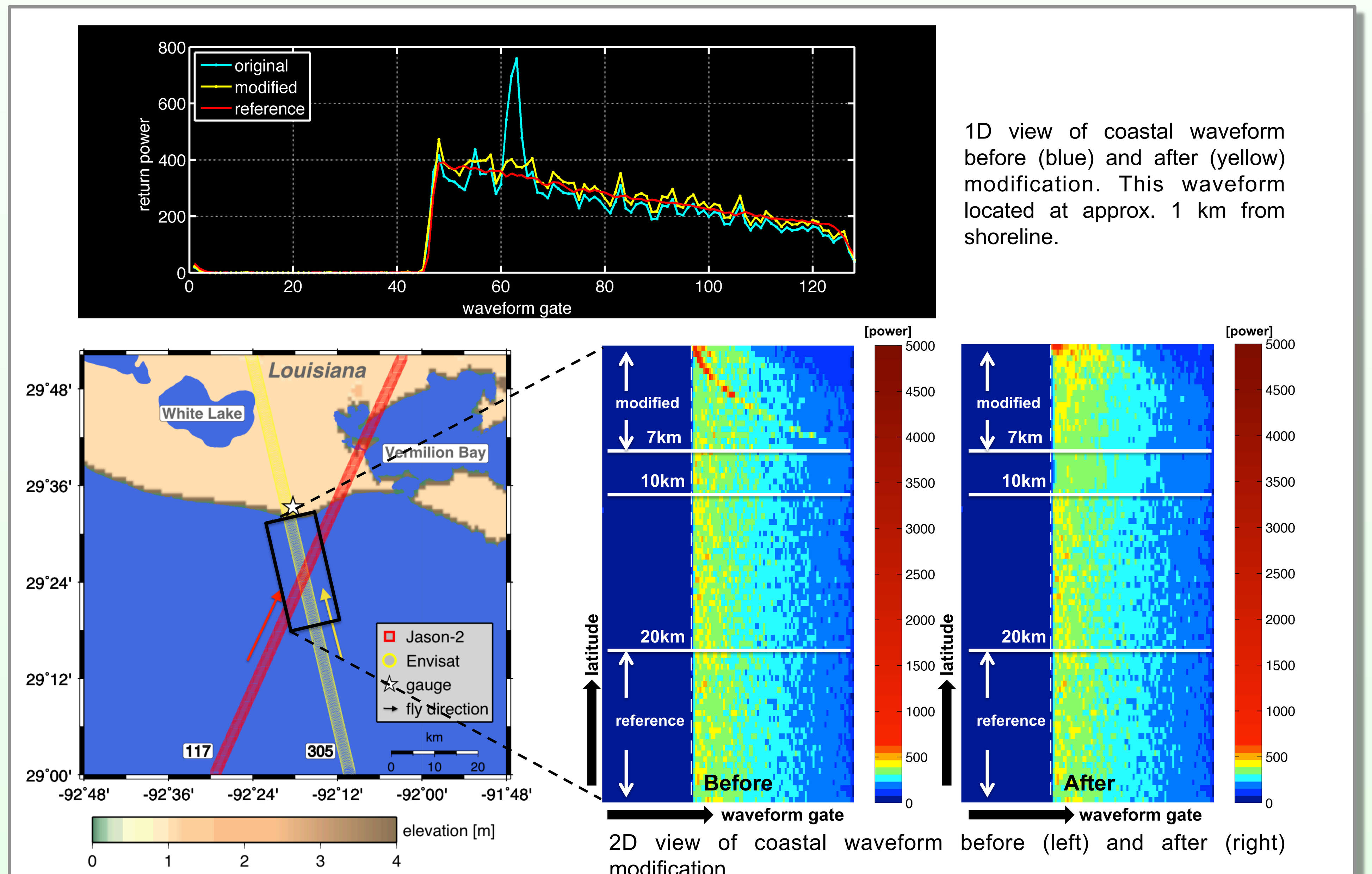

1D view of coastal waveform before (blue) and after (yellow) modification. This waveform located at approx. 1 km from shoreline.

2D view of coastal waveform before (left) and after (right) modification

Figure 2. Waveform modification exemplified by Envisat pass near Louisiana coastal region

4. Results

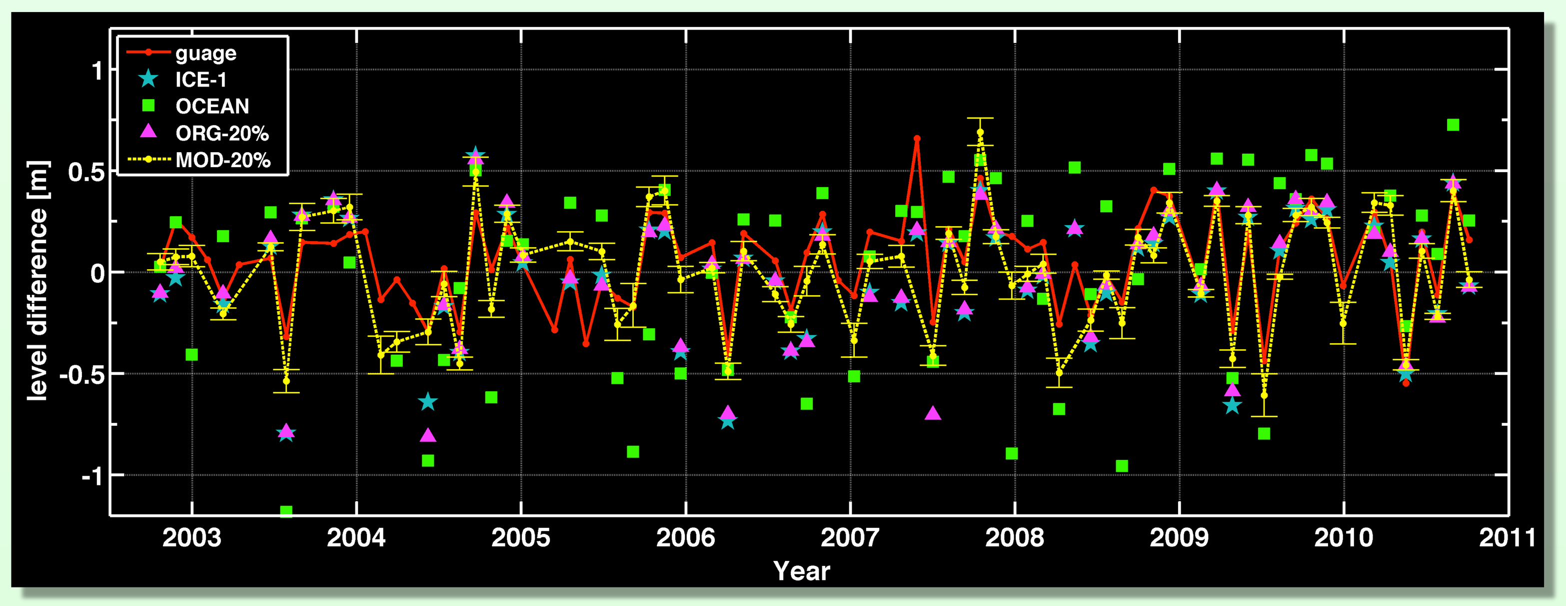

Figure 3. Water level difference compared by tide gauge (red) and various retrackers: ICE-1 (blue), OCEAN (green), 20% threshold to original waveform (magenta), and 20% threshold to modified waveform (yellow).

Fig.3 indicates that modifying waveforms allow one to better recover surface height particularly when the sea level is lower, which resulted in a wider exposure of the shoreline causing stronger land contamination to the original waveform. The peaks after the nominal tracking gate in the original waveform make the range corrections longer. Based on the statistics (Table 1) we conclude that retracking using modified waveforms outperform in most cases, regardless of de-outlier process using gauge data. Also, since the empirical threshold retracking is a data-flag-free method, even if the waveform are incompatible with Brown's model, we can still calculate retracked height without auxiliary environmental variables. Accordingly, advantages in using modified waveforms include: 1. better opportunity to obtain more data at coastal region under conventional data editing criteria, 2. less data gaps in the time series, and 3. better or at least comparable estimates with other existing retrackers used on original waveforms.

Case 1: Alaska

satellite and retracker		include flag			exclude flag			data #	flag #[3]	flag %
		before de-out [m]	after de-out [m]	outlier #[1]	before de-out [m]	after de-out [m]	outlier #[1]			
Envisat 221	ICE-1	>10	0.12	24	>10	0.14	22	5765	82	1.42
	OCEAN	>10	0.11	32	>10	**0.13**	25	5765	73	1.27
	MOD-20%[4]	N/A[2]	N/A[2]	N/A[2]	>10	0.38	34	5765	-	-
	ORG-20%[5]	N/A[2]	N/A[2]	N/A[2]	>10	0.20	28	5765	-	-
Jason-2 130	ICE-1	1.00	0.29	16	1.00	0.29	16	9621	0	0.00
	OCEAN	>10	>10	0	2.67	1.76	5	9621	1427	14.83
	MOD-20%[4]	N/A[2]	N/A[2]	N/A[2]	**0.72**	**0.28**	14	9621	-	-
	ORG-20%[5]	N/A[2]	N/A[2]	N/A[2]	1.17	0.36	15	9621	-	-

Case 2: Louisiana

satellite and retracker		include flag			exclude flag			data #	flag #[3]	flag %
		before de-out [m]	after de-out [m]	outlier #[1]	before de-out [m]	after de-out [m]	outlier #[1]			
Envisat 305	ICE-1	1.08	0.17	20	1.08	0.17	20	6105	0	0.00
	OCEAN	0.69	0.36	10	0.69	0.36	10	6105	0	0.00
	MOD-20%[4]	N/A[2]	N/A[2]	N/A[2]	**0.48**	**0.13**	9	6105	-	-
	ORG-20%[5]	N/A[2]	N/A[2]	N/A[2]	1.04	0.18	19	6105	-	-
Jason-2 117	ICE-1	0.36	0.20	3	0.36	**0.20**	3	11045	0	0.00
	OCEAN	>10	>10	0	1.05	1.05	1	11045	1045	9.46
	MOD-20%[4]	N/A[2]	N/A[2]	N/A[2]	**0.32**	0.25	3	11045	-	-
	ORG-20%[5]	N/A[2]	N/A[2]	N/A[2]	0.38	0.24	2	11045	-	-

Case 3: California

satellite and retracker		include flag			exclude flag			data #	flag #[3]	flag %
		before de-out [m]	after de-out [m]	outlier #[1]	before de-out [m]	after de-out [m]	outlier #[1]			
Envisat 027	ICE-1	1.73	0.44	9	1.73	0.44	9	6175	0	0.00
	OCEAN	1.34	0.90	1	**1.34**	0.90	1	6175	0	0.00
	MOD-20%[4]	N/A[2]	N/A[2]	N/A[2]	2.20	**0.14**	11	6175	-	-
	ORG-20%[5]	N/A[2]	N/A[2]	N/A[2]	2.28	0.65	7	6175	-	-
Jason-2 119	ICE-1	0.61	0.14	6	0.61	0.14	6	9587	0	0.00
	OCEAN	>10	>10	3	1.40	0.61	9	9587	854	8.91
	MOD-20%[4]	N/A[2]	N/A[2]	N/A[2]	**0.28**	**0.13**	9	9587	-	-
	ORG-20%[5]	N/A[2]	N/A[2]	N/A[2]	0.68	0.18	11	9587	-	-

Case 4: Florida

satellite and retracker		include flag			exclude flag			data #	flag #[3]	flag %
		before de-out [m]	after de-out [m]	outlier #[1]	before de-out [m]	after de-out [m]	outlier #[1]			
Envisat 140	ICE-1	0.28	0.28	0	**0.28**	0.28	0	6091	0	0.00
	OCEAN	0.33	0.33	0	0.33	0.33	0	6091	0	0.00
	MOD-20%[4]	N/A[2]	N/A[2]	N/A[2]	1.51	**0.27**	2	6091	-	-
	ORG-20%[5]	N/A[2]	N/A[2]	N/A[2]	1.50	0.28	1	6091	-	-
Jason-2 102	ICE-1	0.84	0.70	2	0.84	0.70	2	11039	0	0.00
	OCEAN	>10	1.36	36	1.82	1.82	0	11039	755	6.84
	MOD-20%[4]	N/A[2]	N/A[2]	N/A[2]	**0.37**	**0.36**	1	11039	-	-
	ORG-20%[5]	N/A[2]	N/A[2]	N/A[2]	0.92	0.79	2	11039	-	-

Table 1. Statistics of selected retrackers compared with tide gauge data. The best estimates are indicated by bold numbers in each study region.

Note:
1. outliers are defined by (retracked - gauge) > 2σ
2. threshold retracking is an empirical method with no pre-defined flags
3. total flag number at coastal region (<7km) in all cycles
4. 20% threshold retracking to modified waveform
5. 20% threshold retracking to original waveform

Acknowledgement

This research is partially supported by NASA OSTST under Grant No. NNX08AR61G (PI. W. Emery, U. Colorado), & a student travel grant by NOAA/CIOSS.
Laury Miller (NOAA/NESDIS/STAR/LSA)
Ted Strub (OSU/COAS/CIOSS)
Amy Vandehey (OSU/COAS/CIOSS)

References

Brown, G.S. (1977), The average impulse response of a rough surface and its applications, *IEEE Trans. Antennas Propag.*, 25(1):67–74.

Calmant, S., F. Seyler, and J. F. Cretaux (2008), Monitoring continental surface waters by satellite altimetry, *Surv. Geophys.*, 29(4–5), 247–269, doi: 10.1007/s10712-008-9051-1.

Kuo, Chung-Yen, Huan-Chin Kao. (2011), Retracked Jason-2 Altimetry over Small Water Bodies: Case Study of Bajhang River, Taiwan. *Marine Geodesy* 34:3-4, 382-392.

Fu, L. L., and A. Cazenave (2001), Satellite aAltimetry and Earth Sciences, A Handbook of Techniques and Applications, International Geophysics Series, 69, Academic Press, San Diego, Calif.

Lee, H.K., C.K. Shum, Y. Yi, A. Braun, and C.Y. Kuo. (2008), Laurentia Crustal Uplift Observed Using Satellite Radar Altimetry, *J. Geodyn.,* 46:182-193.

Lee, H. K., C.K. Shum, W. Emery, S. Calmant, X. Deng, C. Y. Kuo, C. Roesler, Y. Yi, (2010), Validation of Jason-2 altimeter data by waveform retracking over California coastal ocean, *Marine Geodesy*, 33(S1): 304–316, doi: 10.1080/01490419.2010. 488982.

OSTM/Jason-2 Products Handbook. 2009. JPL. OSTM-29-1237.